This is an *Accepted Manuscript*, which has been through the Royal Society of Chemistry peer review process and has been accepted for publication.

Accepted Manuscripts are published online shortly after acceptance, before technical editing, formatting and proof reading. Using this free service, authors can make their results available to the community, in citable form, before we publish the edited article. We will replace this *Accepted Manuscript* with the edited and formatted *Advance Article* as soon as it is available.

You can find more information about *Accepted Manuscripts* in the **Information for Authors**.

Please note that technical editing may introduce minor changes to the text and/or graphics, which may alter content. The journal's standard **Terms & Conditions** and the **Ethical guidelines** still apply. In no event shall the Royal Society of Chemistry be held responsible for any errors or omissions in this *Accepted Manuscript* or any consequences arising from the use of any information it contains.

Journal Name

ARTICLE

Synthesis and magnetic properties of tartrate-bridging rare-earth-containing polytungstoarsenate aggregates from an adaptive precursor $[As_2W_{19}O_{67}(H_2O)]^{14-}$

Yuan Wang,[a] Xiaopeng Sun,[a] Suzhi Li,[b] Pengtao Ma,[a] Jingping Wang,*[a] Jingyang Niu*[a]

Six tartrate-bridging rare-earth-substituted polytungstoarsenates $[RE_2(C_4H_4O_6)(C_4H_2O_6)(AsW_9O_{33})]_2^{18-}$ (Ho[III] (**1**), Er[III] (**2**), Tm[III] (**3**), Yb[III] (**4**), Lu[III] (**5**), Y[III] (**6**)) have been synthesized under conventional solution conditions. They have been further characterized by elemental analyses, X-ray powder diffraction (XRPD), IR spectra, UV-vis spectra and single-crystal X-ray diffraction. Preliminary variable-temperature magnetic susceptibility measurements indicate that **1**–**4** exhibit the antiferromagnetic coupling.

Introduction

Polyoxometalates (POMs), an important class of inorganic compounds displaying various compositional range and significant structural diversity,[1] have attracted increasing interest owing to their potential applications in different fields such as materials science,[2] medicine,[3] catalysis,[2] electrochemistry[4] and magnetic chemistry.[5] However, the formation mechanism of POMs is still not well understood and commonly described as self-assembly. Thus, the design of elaborate POMs remains a challenge. Generally speaking, two strategies, straightforward synthesis and building block approach, have been developed to prepare novel POMs. It is considered that straightforward synthesis is a self-assembly process that mononuclear oxoanions (like WO_4^{2-}, MoO_4^{2-}) aggregate into polynuclear POMs including the large and giant species at suitable pH.[6] Hitherto, many polynuclear POMs, such as tungstate $\{W_{148}\}$[7] and the largest molybdate $\{Mo_{368}\}$[8], were obtained by a straightforward "one-pot" synthesis via the self-assembly process. However, the unpredictability and uncontrollability of the product confine its development. On the contrary, the building block approach keeps expanding the arsenal of new POM-based complexes via step-by-step control of aggregation process. It allows the chemists to fine-tune the reaction and create a large number of new compounds with purposeful actions. Therefore, the building block approach is deemed to be a more effective and feasible method to isolate target product especially for polyoxotungstates.[9] As for this strategy, vacant Keggin-type and Dawson-type polyoxoanions were extensively used as the building blocks and linked by metal cations in different ways to form various structural topologies from isolated clusters[9b,10] to chainlike aggregates.[11] Nevertheless, the dilacunary species $[As_2W_{19}O_{67}(H_2O)]^{14-}$ firstly draws our attention as compared with the classical defect POMs for the reasons below: (1) the $\{WO(H_2O)\}$ linker between two $[B-\alpha-AsW_9O_{33}]^{9-}$ could serve as a starting point for rotation and dissociation, which may facilitate the generation of a number of building blocks in solution at different pH;[12] (2) the stereodirecting influence of lone pair on the As[III] atom guarantees the emergence of the lacunary building blocks, resulting in a very different reactivity compared with vacant POMs with tetrahedral hetero groups[1b]; (3) it is easy to prepare the precursor. It's our understanding that several RE-containinng arsenotungstates have been isolated based on the $[As_2W_{19}O_{67}(H_2O)]^{14-}$ including: $[Gd_8As_{12}W_{124}O_{432}(H_2O)_{22}]^{60-}$,[10] $[Tb_2(pic)(H_2O)_2(B-\beta-AsW_8O_{30})_2(WO_2(pic))_3]^{10-}$,[12] $[Tb_8(pic)_6(H_2O)_{22}(B-\beta-AsW_8O_{30})_4(WO_2(pic))_6]^{12-}$,[12] $[Ln_{16}As_{16}W_{164}O_{576}(OH)_8(H_2O)_{42}]^{80-}$,[9c] $Li_8[Ln_4As_5W_{40}O_{144}(H_2O)_{10}(Gly)_2]\cdot25H_2O$.[13] But, most of the previous reports on RE-containinng arsenotungstates are purely inorganic or they contain monocarboxylic ligands (such as glycine, pyridine-2-carboxylic acid), little work has been devoted to arsenotungstates containing rare earth metals and multicarboxylic ligands, simultaneously. Therefore, it is still meaningful and challenging to synthesize new complexes in this family starting from the $[As_2W_{19}O_{67}(H_2O)]^{14-}$. Herein, we choose racemic tartaric acid as the polyfunctional bridging ligand on the basis of the following interesting characteristics: (1) Among the extensive library of this type of ligand, tartaric acid appears to be largely undeveloped with only a few examples of TM-coordination POMs[14] and no example of RE-containing arsenotungstate has been reported; (2) the carboxylate groups can be completely or partially deprotonated to generate different tartaric acid segments allowing various acidity-dependent coordination modes, which make the ligand polydentate and thus be suitable for leading to a large possibility to construct novel RE-containing POMs; (3) the tartaric acid is a flexible ligand which can act as hydrogen bond donors and/or hydrogen bond acceptors, favoring the construction of supramolecular structures.

In considerations of the above-mentioned factors, the dilacunary POM $[As_2W_{19}O_{67}(H_2O)]^{14-}$ was utilized as the precursor, racemic tartaric acid and rare earth cations as the bridging fragments with the purpose to isolate new POM-based complexes via the building block approach. Fortunately, when mixing the $[As_2W_{19}O_{67}(H_2O)]^{14-}$ with rare earth cations (Ho[III],

Er^{III}, Tm^{III}, Yb^{III}, Lu^{III}, Y^{III}) and tartaric acid molecule, we achieved a new series of polytungstoarsenates (III): K$_{13}$LiH$_4$[RE$_2$(C$_4$H$_4$O$_6$)(C$_4$H$_2$O$_6$)(AsW$_9$O$_{33}$)]$_2$·28H$_2$O (RE = Ho^{III} (1), Er^{III} (2), and K$_9$LiH$_8$[RE$_2$C$_4$H$_4$O$_6$)(C$_4$H$_2$O$_6$)(AsW$_9$O$_{33}$)]$_2$·nH$_2$O (RE = Tm^{III} (3), n = 35, Yb^{III}(4), n = 33, Lu^{III} (5), n = 33, Y^{III} (6), n = 36).

Results and discussion

Synthesis The syntheses of compounds **1–6** were achieved from the reaction of K$_{14}$[As$_2$W$_{19}$O$_{67}$(H$_2$O)] with chlorate salts of Ho^{III}, Er^{III}, Tm^{III}, Yb^{III}, Lu^{III}, Y^{III} and racemic tartaric acid in a molar ratio 5:12:20 in 60°C aqueous solution under stirring for 1 h. Several variables have been investigated in our work such as pH, organic components and molar ratio *etc*. First, of importance in the preparation of compounds **1–6**, is the introduction of excess tartaric acid. Its presence during the synthesis is crucial because replacement of tartaric acid by hexane diacid, glutaric acid or succinic acid does not result in the desired product. To the best of our knowledge, tartaric acid as a multidente oxygen-donor organic ligand is a perfect candidate to investigate the possibility of synthesizing RE-POM cluster species, as it is effective at stabilizing rare earth metals even in high pH aqueous solutions. This essential property has prompted us to explore its effects as a structure directing reagent and one reactant in this reaction system. In fact, other polycarboxylic acids such as malonic acid, hexane diacid, glutaric acid and succinic acid have also been used, to our regret, only can we obtain some precipitation rather than monocrystal samples, which may be ascribed to their weaker complexation compared to tartaric acid. In addition, if the tartaric acid is added in stoichiometric amount, some precipitate will form resulting in the low yield. Therefore, it is supposed that the excess tartaric acid might serve as a buffer and provide a mild environment for the POMs and rare earth metals, preventing them from precipitating. This phenomenon is similar to the citric acid reported by Xu's group.[15] In particular, it is essential for the reaction to conduct at suitable pH. Parallel experiments confirm that the crystals of compounds **1–6** can just be isolated in the pH range of 5.5–6.5, and the higher the pH is, the lower the yield.

Structural descriptions
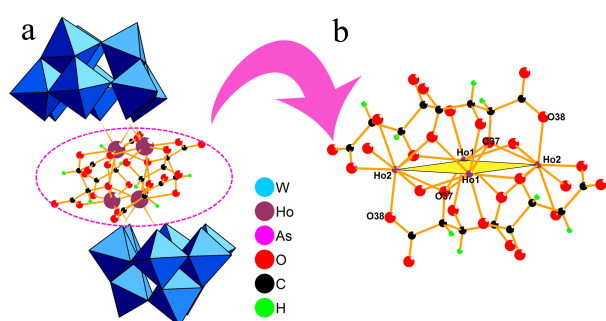
Figure 1. (a) Polyhedral/ball-and-stick representation of the structural unit of compound **1**; (b) the metal oxide cluster in compound **1**.

Bond valence sum calculations[16] indicate that all W atoms, As atoms and RE atoms in **1–6** are in the +6, +3 and +3 oxidation states, respectively. For each compound of the six, a lithium ion is added based on elemental analysis. In consideration of the balance of the charge state, four hydrogen ions need to be

added for **1**, **2** and eight hydrogen ions for **3**, **4** and **5**. The RE–O bond lengths (Table S1 in the electronic supplementary information) almost decrease as the ionic radius of the RE^{III} cations decrease, which is in accordance with the effect of the lanthanide contraction. Single crystal X-ray diffraction analyses reveal that compounds **1–6** crystallize in the triclinic space group *P-1* and contain similar polyanions [RE$_2$(C$_4$H$_4$O$_6$)(C$_4$H$_2$O$_6$)(AsW$_9$O$_{33}$)]$_2^{18-}$ (Figure 1a), which are connected by K$^+$ resulting in the 3D framework (Figure 2). Herein, only a case of compound **1** is illustrated in the following description.
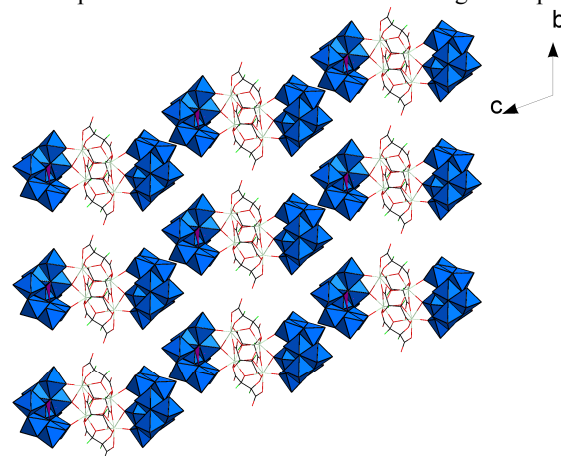
Figure 2. Packing of the POM in compound **1** viewed along a axis (K+ and H$_2$O are omitted for clarity).

The polyanion of compound **1** is composed of two B-α-{AsW$_9$O$_{33}$} units opposed to each other sandwiching a unique cage-like metal-oxide moiety and possessed an "S-shaped" structure, where the cage-like metal-oxide cluster is constituted by four lanthanide cations and four tartaric acid segments. In the cluster, the metal-oxide fragment acting as a bridge connects the two {AsW$_9$O$_{33}$} units together. Subtly, the four rare earth cations of the metal-oxide fragment are in a parallelogram plane (Figure 1b). Of the four rare earth cations, the two cations located on the same diagonal are crystallographically equivalent and the four rare earth cations are subdivided into two categories: Ho1 and Ho2. The eight-coordinate center Ho1 and Ho2 could be considered as the hinges linking the metal-oxide fragment and two{AsW$_9$O$_{33}$} subunits together *via* two Ho–O(W) bonds, six Ho–O(C) bonds exhibiting distorted dodecahedral coordination geometry (Ho1–O: 2.219(10)–2.453(11) Å; Ho2–O: 2.271(12)–2.494(11) Å) (Figure 3). It should be mentioned that the tartaric acid molecules have unusual chelation modes. There are two non-equivalent tartaric acid segments above/below the plane. The first tartaric acid pieces bridge two rare earth ions simultaneously, exploiting an unusual μ_2: μ_2: μ_3: μ_2 fashion.
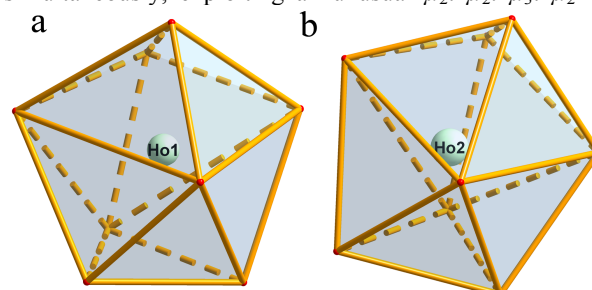
Figure 3. (a) The coordination environment of the Ho1^{3+}; (b) the coordination environment of the Ho2^{3+}.

While the other one just like an adhesive chelates three lanthanide ions concurrently, employing μ_3: μ_2: μ_4: μ_2 mode. Other else, μ_4-O37 and μ_2-O38 of the latter tartaric acid are monoprotonated, but no atom is observed as protonated according to bond value calculations. As far as we know, such two coordination modes of tartrate ligand are seldom reported. In a word, those two uncommon coordination modes may be two key factors in providing the strong complexation between tartaric acid segments and the large metal-oxide framework. And the complexation in turn dictates the configurational stability of the compounds **1**–**6**.

XRPD and FT-IR Patterns

The XRPD patterns for compounds **1**–**6** are presented in Figure S1. The diffraction peaks of simulated patterns do not completely match with experimental patterns because the samples of **1**–**6** have badly weathered before the XRPD experiments. The differences in intensity may be due to the preferred orientation of the powder samples.

The peak shapes of the IR spectra in the 400−3500 cm^{-1} region of **1**−**6** are similar (Figure S2), indicating the polyanions in **1**−**6** are isostructure. Broad peaks at 3435 cm^{-1} and 1615 cm^{-1} are attributed to the stretching and bending modes of lattice and coordinated water molecules. The peaks at 1395 cm^{-1} may correspond to the vibration of carboxyl group. The stretching vibration of C–O (RE) may be responsible for the peaks at 1081 cm^{-1}. A characteristic peak for the polyanion at 943 cm^{-1} can be assigned to the W=O stretching vibration and peaks at 889 cm^{-1}, 747 cm^{-1} and 802 cm^{-1} belong to the two types of W–O–W stretching vibrations, and the peak at 703 cm^{-1} can be assigned to the W–O(As) stretch. [13]

UV Spectra

The UV spectra of compounds **1**–**6** (5×10^{-5} mol·L^{-1}) in aqueous solution display two absorption bands at 200 nm and 250–254 nm (Figure S3). The former higher energy band can be assigned to the pπ-dπ charge-transfer transitions of the O$_t$→W band, whereas the latter lower one could be attributed to the pπ-dπ charge-transfer transitions of the O$_{b,c}$→W bands, indicating the formation of polyoxoanions. [17] In order to investigate the stability of the solution of **1**–**6**, the in-situ spectroscopic measurements were performed in the aqueous system. Both the position and the strength of the absorption bands of compounds **1**–**6** are not change indicating that compounds **1**–**6** may be stable in the aqueous system at ambient temperature at 5 hours.

It is well known that the POMs are commonly sensitive to the pH value of the studied media. Therefore, in order to investigate the influences of the pH values on the stability of compounds in aqueous solution, **3** have been elaborately probed by means of UV-vis spectra. Diluted HCl solution and LiOH solution were used to adjust the pH values in the acidic direction and in the alkaline direction, respectively. The initial pH value of **3** in water was 4.6. As indicated in Figure S4, the UV spectrum of **3** in aqueous solution displays two absorption bands at 200 and 252 nm and the UV spectrum of **3** is not change at all even the pH value has been lowered to 1.6. In contrast, when increasing the pH value of **3**, the absorbance band at 252 nm is gradually blue-shifted and becomes weaker and weaker, suggesting the decomposition of the POM skeleton of **3**. [18] This phenomenon is especially obvious when the pH is higher than 9.6, which indicate that the POM skeleton of **3** is destroyed at pH higher than 9.6. The results above have told us

that compound **3** could not exist in the solution whose pH is higher than 9.6.

Magnetic properties
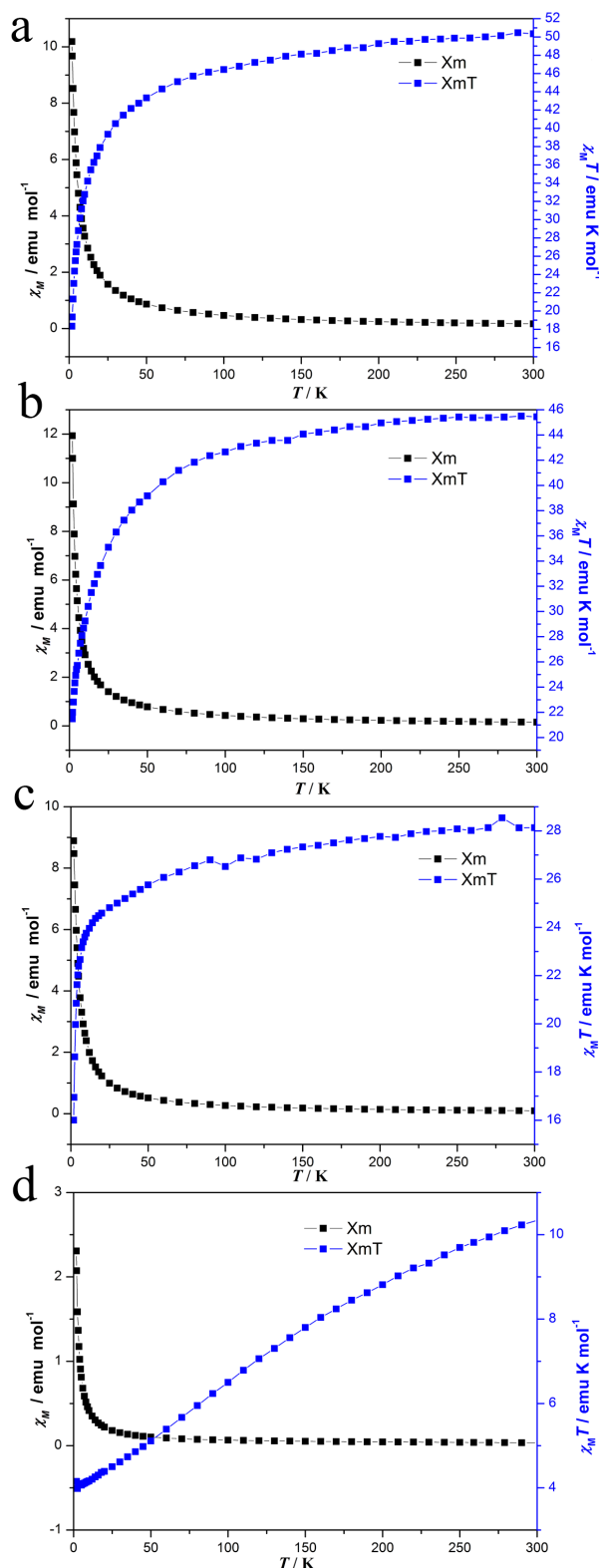
Figure 4. Plots of χ_M and $\chi_M T$ vs T for **1**(a), **2**(b), **3**(c), **4**(d).

Generally speaking, the spin-orbital coupling plays a more important role in the magnetism of lanthanide complexes

compared with crystal field.[19] This spin-orbital coupling leads to the $4f^n$ configuration of Ln^{III} ions, except for Gd^{III}, to split

Table 1. Crystallographic Data for **1–6**.

	1	**2**	**3**	**4**	**5**	**6**
Formula	$C_{16}H_{72}As_2Ho_4$ $LiK_{13}O_{118}W_{18}$	$C_{16}H_{72}As_2Er_4$ $LiK_{13}O_{118}W_{18}$	$C_{16}H_{90}As_2Tm_4$ $LiK_9O_{125}W_{18}$	$C_{16}H_{86}As_2Yb_4$ $LiK_9O_{123}W_{18}$	$C_{16}H_{86}As_2Lu_4$ $LiK_9O_{123}W_{18}$	$C_{16}H_{92}As_2Y_4$ $LiK_9O_{126}W_{18}$
Mr (g.mol^{-1})	6786.58	6795.89	6776.34	6756.72	6764.44	6474.24
T (K)	296(2)	296(2)	296(2)	296(2)	296(2)	296(2)
Crystal system	Triclinic	Triclinic	Triclinic	Triclinic	Triclinic	Triclinic
Space group	*P-1*	*P-1*	*P-1*	*P-1*	*P-1*	*P-1*
a (Å)	11.9933(11)	11.9777(11)	11.939(3)	11.8725(7)	11.879(3)	11.9045(12)
b (Å)	15.2025(13)	15.1643(14)	16.657(4)	16.5529(9)	16.555(4)	16.6180(17)
c (Å)	19.8114(17)	19.7826(18)	17.412(4)	17.2796(10)	17.280(4)	17.4108(17)
α (deg)	105.2820(10)	105.2430(10)	98.755(4)	98.6930(10)	98.673(4)	98.786(2)
β (deg)	101.371(2)	101.4070(10)	99.642(4)	99.7480(10)	99.747(4)	99.420(2)
γ (deg)	107.5420(10)	107.654(2)	90.097(4)	90.1770(10)	90.172(4)	90.080(2)
V (Å^3)	3168.6(5)	3149.4(5)	3372.5(13)	3307.0(3)	3308.5(13)	3356.8(6)
Z	1	1	1	1	1	1
Dc (g. cm^{-3})	3.549	3.575	3.230	3.302	3.303	3.086
μ (mm^{-1})	19.786	20.059	18.746	19.263	19.405	17.928
Limiting indices	$-14 \leq h \leq 14$, $-16 \leq k \leq 18$, $-23 \leq l \leq 18$	$-14 \leq h \leq 14$, $-17 \leq k \leq 18$, $-23 \leq l \leq 19$	$-14 \leq h \leq 14$, $-19 \leq k \leq 14$, $-20 \leq l \leq 20$	$-14 \leq h \leq 14$, $-19 \leq k \leq 19$, $-20 \leq l \leq 19$	$-14 \leq h \leq 14$, $-17 \leq k \leq 19$, $-20 \leq l \leq 20$	$-14 \leq h \leq 14$, $-19 \leq k \leq 19$, $-20 \leq l \leq 15$
Params	466	466	432	434	439	433
Reflns collected	16247	16204	17329	17030	17010	17081
GOF	1.020	1.004	1.030	1.037	1.036	1.027
R$_1$, wR$_2$ [I>2σ(I)]	0.0483, 0.1185	0.0401, 0.0990	0.0524, 0.1416	0.0461, 0.1185	0.0480, 0.1269	0.0554, 0.1484
R$_1$, wR$_2$ [all data]	0.0671, 0.1294	0.0491, 0.1040	0.0702, 0.1546	0.0600, 0.1270	0.0631, 0.1371	0.0845, 0.1669

into $^{2S+1}L_J$ states, and the latter further splits into Stark components under the crystal-field perturbation.[19] Thus, the variable-temperature magnetic properties of a free ion of a metal shows strong deviations from the Curie law, and $\chi_M T$ decreases with the cooling temperature because of the depopulation of Stark levels.[20] Although the theory of the paramagnetic properties of lanthanide cations has long been investigated, the presence of the large unquenched orbital angular momentum has not allowed the development of simple models for a rational analysis of the structural magnetic correlations, which makes the analysis of the experimental data more difficult.[20] Herein, variable-temperature magnetic susceptibility measurements of **1–4** have been performed in the range of 1.8–300K at an applied field of 2kOe and the results display that the magnetic properties of **1–3** are similar while **4** is somewhat different (Figure 4 and Figure S5).

Compounds **1–3** exhibit similar magnetic properties showing antiferromagnetic coupling between lanthanide ions. As an example, only compound **1** is discussed. For compound **1**, the $\chi_M T$ value slowly decreases from 50.35 emu K mol^{-1} at 300K (Figure 4a), which is lowered than four free Ho^{III} cations (56.67 emu K mol^{-1}, g = 5/4). [20b, 20c] Once the temperature is lowered than 20 K, the $\chi_M T$ value reduces drastic and down to 18.34 emu K mol^{-1} at 1.8 K, exhibiting antiferromagnetic coupling with $C = 50.89$ emu K mol^{-1}, and $\theta = -6.43$ K (Figure S5a).

Compound **4** exhibits magnetic properties which is very different from that of compound **1–3** as elaborated in Figure 4d. As for compound **4**, at 300 K, the $\chi_M T$ is equal to 10.36 emu K mol^{-1} that is somewhat higher than the theoretical value of 10.28 emu K mol^{-1} based on four independent Yb^{III} ions with $^2F_{7/2}$ ground multiplet,[19c, 20a] and it almost monotonically decreases to 4.15 emu K mol^{-1} at 1.8K, suggesting that the depopulation of the Stark levels possibly dominates the magnetic behaviors in compound **4**. As a result, compound **4** does not obey Curie-Weiss law (Figure S5d), which is similar with the compound $[Yb_2(L)(HL)(NO_3)_6(HCOO)]$ $3CH_3OH$.[20a]

Experimental section

General methods and materials

$K_{14}[As_2W_{19}O_{67}(H_2O)]$ was prepared according to Kortz[9b] and conformed by IR spectrum. Other chemical reagents were purchased and used without further purification. Elemental analyses (C, H) were conducted on a Perkin-Elmer 2400–II CHNS/O analyzer. IR spectra were recorded on a Bruker VERTEX 70 IR spectrometer using KBr pellets in the range of 4000–400 cm^{-1}. ICP analyses were performed on a Perkin-Elmer Optima 2000 ICP–OES spectrometer. UV-vis absorption spectra were obtained with a U–4100 spectrometer at room temperature. XRPD experiments were performed on Bruker AXS D8 Advance diffractometer instrument with Cu Kα radiation (λ = 1.54056 Å) in the range 2θ = 5–45° at 293K. The magnetic data were collected on Quantum Design SQUID (MPMS-XL7).

Synthesis of $K_{13}H_4Li[Ho_2(C_4H_4O_6)(C_4H_2O_6)(AsW_9O_{33})]_2 \cdot 28 H_2O$ (1) The representative synthesis of compound 1 was

performed as follows: a sample of $K_{14}[As_2W_{19}O_{67}(H_2O)]$ (0.658g, 0.125mmol) was added under stirring to a solution of 0.075g tartaric acid (0.50mmol) and $HoCl_3 \cdot 6H_2O$ (0.30mmol, 0.114g) in 15mL water, ten minutes later, the pH of the solution was adjusted to about 5.5 with $1.00 \text{ mol} \cdot L^{-1}$ lithium hydroxide and then the mixture was heated to 60°C for 1h. After being cooled to room temperature, the clear solution was stood for crystallization. Colorless and block crystals were collected after about two weeks. The crystals must be stilled in a capillary tube as the crystals are easy to weathering when prepared for X-ray crystal structure determination. Yield: 0.10g (19.67 % based on $HoCl_3 \cdot 6H_2O$). Elemental analysis (%) calcd for **1**: C, 2.83; H, 1.07; K, 7.49; Li, 0.10; Ho, 9.72; As, 2.21; W, 48.76. Found: C, 2.76; H, 1.16; K, 7.61; Li, 0.11; Ho, 9.91; As, 2.23; W, 49.13. Selected IR (KBr, cm^{-1}): 3435 (br), 1615 (s), 1395 (w), 1255 (w), 1202 (w), 1081 (w), 943 (s), 889 (s), 802 (s), 747 (s), 703 (w).

Synthesis of $K_{13}H_4Li[Er_2(C_4H_4O_6)(C_4H_2O_6)(AsW_9O_{33})]_2 \cdot 28 H_2O$ (2) The synthesis of **2** is similar with **1** but with $ErCl_3 \cdot 6H_2O$ (0.30mmol, 0.115g) instead of $HoCl_3 \cdot 6H_2O$. Yield: 0.09g (17.68 % based on $ErCl_3 \cdot 6H_2O$). Elemental analysis (%) calcd for **2**: C, 2.83; H, 1.07; K, 7.48; Li, 0.10; Er, 9.84; As, 2.20; W, 48.69. Found: C, 2.76; H, 1.20; K, 7.39; Li, 0.11; Er, 10.00; As, 2.16; W, 48.92. Selected IR (KBr, cm^{-1}): 3435 (br), 1613 (s), 1400 (s), 1253 (w), 1209 (w), 1087(w), 940 (s), 890 (s), 801 (s), 742 (s), 698 (w).

Synthesis of $K_9H_8Li[Tm_2(C_4H_4O_6)(C_4H_2O_6)(AsW_9O_{33})]_2 \cdot 35 H_2O$ (3) The synthesis of **3** is similar with **1** but with $TmCl_3 \cdot 6H_2O$ (0.30mmol, 0.115g) instead of $HoCl_3 \cdot 6H_2O$. Yield: 0.11g (21.58 % based on $TmCl_3 \cdot 6H_2O$). Elemental analysis (%) calcd for **6**: C, 2.84; H, 1.34; K, 5.19; Li, 0.10; Tm, 9.97; As, 2.21; W,48.83. Found: C, 2.89; H, 1.26; K, 5.15; Li, 0.11; Tm, 9.82; As, 2.14; W, 48.90. Selected IR (KBr, cm^{-1}): 3435 (br), 1610 (s), 1397 (s), 1255 (m), 1209 (w), 1088 (w), 940 (s), 891 (s), 800 (s), 746 (s), 704 (w).

Synthesis of $K_9H_8Li[Yb_2(C_4H_4O_6)(C_4H_2O_6)(AsW_9O_{33})]_2 \cdot 33 H_2O$ (4) The synthesis of **4** is similar with **1** but with $YbCl_3 \cdot 6H_2O$(0.30mmol, 0.116g) instead of $HoCl_3 \cdot 6H_2O$. Yield: 0.08g (15.67 % based on $YbCl_3 \cdot 6H_2O$). Elemental analysis (%) calcd for **4**: C, 2.84; H, 1.28; K, 5.21; Li, 0.10; Yb, 10.24; As, 2.22; W, 50.18. Found: C, 2.92; H, 1.17; K, 5.26; Li, 0.10; Yb, 10.18; As, 2.30; W,49.89. Selected IR (KBr, cm^{-1}): 3435 (br), 1617 (s), 1399 (w), 1255 (w), 1209 (w), 1088 (w), 940 (s), 890 (s), 799 (s), 751 (s), 698 (w).

Synthesis of $K_9H_8Li[Lu_2(C_4H_4O_6)(C_4H_2O_6)_2(AsW_9O_{33})]_2 \cdot 33 H_2O$ (5) The synthesis of **5** is similar with **1** but with $LuCl_3 \cdot 6H_2O$ (0.30mmol, 0.117g) instead of $HoCl_3 \cdot 6H_2O$. Yield: 0.09g (17.60 % based on $LuCl_3 \cdot 6H_2O$). Elemental analysis (%) calcd for **5**: C, 2.84; H, 1.28; K, 5.20; Li, 0.10; Lu, 10.34; As, 2.22; W, 50.12. Found: C, 2.77; H, 1.30; K, 5.18; Li, 0.11; Lu, 10.43; As, 2.14; W, 49.98. Selected IR (KBr, cm^{-1}): 3435 (br), 1610 (s), 1399 (w), 1255 (s), 1209 (s), 940(s), 890 (s), 799 (s), 747 (s), 697 (w).

Synthesis of $K_9H_8Li[Y_2(C_4H_4O_6)(C_4H_2O_6)(AsW_9O_{33})]_2 \cdot 36 H_2O$ (6) The synthesis of **6** is similar with **1** but with $YCl_3 \cdot 6H_2O$ (0.30mmol, 0.091g) instead of $HoCl_3 \cdot 6H_2O$. Yield: 0.07g (14.40 % based on $YCl_3 \cdot 6H_2O$). Elemental analysis (%) calcd for **6**: C, 2.97; H, 1.43; K, 5.43; Li, 0.11; Y, 5.49; As, 2.31; W, 51.11. Found: C, 3.04; H, 1.36; K, 5.51; Li, 0.11; Y,

5.39; As, 2.24; W, 51.31. Selected IR (KBr, cm^{-1}): 3435 (br), 1611 (s), 1397 (s), 1253 (s), 1210 (s), 1086 (w), 940 (s), 890 (s), 803 (s), 749 (s), 703 (w).

X-ray Crystallography. Single crystals for X-ray structure analysis were performed on Bruker CCD Apex-II diffractometer with Mo Kα radiation (λ = 0.71073Å) at 296K. Routine Lorentz polarization and empirical absorption corrections were applied. The structures of compound **1–6** were solved by direct methods refined by full-matrix least-squares refinements on F^2 using the SHELXL-97 software and an absorption correction was performed using the SADABS program. [21] In the final refinement, the W, As, lanthanoid, and K atoms were refined anisotropically; the O and C atoms were refined isotropically. The amount of lithium ions was determined based on elemental analysis results. The hydrogen atoms of the tartaric acid groups were placed in calculated positions and then refined using a riding model. All H atoms on water molecules were directly included in the molecular formula. The crystallographic data **1–6** are given in Table 1.

Conclusions

In summary, six lanthanoid-based arsenotungstates have been obtained by the building block approach. Furthermore, the magnetic behaviors of **1–4** have been investigated. The work has just proved that the polyanion precursor $[As_2W_{19}O_{67}(H_2O)]^{14-}$ is a superexcellent starting material for the synthesis of elaborate POMs. In the following work, we will introduce different polycarboxylate ligands into the present system and attempt to explore the role of the organic ligands in the reactions.

Acknowledgements

Notes and references

[a] Henan Key Laboratory of Polyoxometalate, Institute of Molecular and Crystal Engineering, College of Chemistry and Chemical Engineering, Henan University, Kaifeng 475004, Henan, China. E-mail: jpwang@henu.edu.cn, jyniu@henu.edu.cn, Fax: (+86) 37123886876.

[b] College of Chemistry and Chemical Engineering, Engineering Research Center of Functional Material Preparation, Shangqiu Normal University, Shangqiu, 476000, Henan, China.

† Electronic supplementary information (ESI) available: XPRD patterns of **1–6** (Figure S1); IR spectra of **1–6** (Figure S2); The UV-vis spectra of **1**(a), **2**(b), **3**(c), **4**(d), **5**(e), **6**(f) with 5×10^{-5} mol/L in aqueous solution(Figure S3); the UV-vis spectra of **3** at different pH values(Figure S4); the χ_M^{-1} vs T curves of **1–4** (Figure S5), CCDC reference numbers 987821–987826 for **1–6**, respectively; the RE–O bond lengths in compounds **1–6** (Table S1). These data can be obtained free of charge from The Cambridge Crystallographic Data Centre via www.ccdc.cam.ac.uk/data_ request/cif.

1 (a) F. Hussain, B. S. Bassil, U. Kortz, O. A. Kholdeeva, M. N. Timofeeva, P. Oliveira, B. Keita, and L. Nadjo, *Chem. Eur. J.,* 2007, **13**, 4733; (b) B. S. Bassil, U. Kortz, *Z. Anorg. Allg. Chem.,* 2010, **636**, 2222; c) A. Dolbecq, E. Dumas, C. R. Mayer, and P. Mialane, *Chem. Rev.*, 2010, **110**, 6009; (d) P. Gouzerh and A. Proust, *Chem. Rev.*, 1998, **98**, 77.

2 (a) Y. F. Song, R. Tsunashima, *Chem. Soc. Rev.,* 2012, **41**, 7384; (b) D. L. Long, R. Tsunashima, Cronin, L. *Angew. Chem. Int. Ed.,* 2010, **49**, 1736; (c) A. Proust, R. Thouvenot, P. Gouzerh, *Chem. Commun.,* 2008, **16**, 1837; (d) V. Duffort, R. Thouvenot, C. Afonso, G. Izzet, A. Proust, *Chem. Commun.,* 2009, **40**, 6062.

3 (a) J. T. Rhule, C. L. Hill, D. Judd, A. *Chem. Rev.,* 1998, **98**, 327; (b) C. L. Hill, M. S. Weeks, R. F. Schinazi, *J. Med. Chem.,* 1990, **33**. 2767; (c) J. Y. Niu, G. Chen, J. W. Zhao, P. T. Ma, S. Z. Li, J. P. Wang, M. X. Li, Y. Bai, B. S. Ji, *Chem. Eur. J.,* 2010, **16**, 7082.

4 (a) M. Sadakane, E. Steckhan, *Chem. Rev.*, 1998, **98**. 219; (b) I. M. Mbomekalle, B. Keita, L. Nadio, P. Berthet, K. I. Hardcastle, C. L. Hill, T. M. Anderson, *Inorg. Chem.,* 2003, **42**, 1163.

5 (a) A. Müller, F. Peter, M. T. Pope, *Chem. Rev.,* 1998, **98**, 239；(b) J.- D. Compain, P. Mialane, A. Dolbecq, I. M. Mbomekallé, J. Marrot, F. Sécheresse, E. Rivière, G. Rogez, W. Wernsdorfer, *Angew. Chem. Int. Ed.,* 2009, **48**, 3077.

6 A. Müller, F. Peters, M. T. Pope and D. Gatteschi, *Chem. Rev.,* 1998, **98**, 239.

7 K. Wassermann, M. H. Dickman, M. T. Pope, *Angew. Chem. Int. Ed.*, 1997, **36**, 1445.

8 A. Müller, E. Beckmann, H. Bögge, M. Schmidtmann, and A. Dress, *Angew. Chem. Int. Ed.,* 2002*,* **41***,* 1162.

9 (a) N. L. Laronze, M. Haouas, J. Marrot, F. Taulelle and G. Hervé, Angew. *Chem., Int. Ed.,* 2006, **45**, 139; (b) U. Kortz, M. G. Savelieff, B. S. Bassil and M. H. Dickman, *Angew. Chem, Int. Ed.,* 2001, **40**, 3384; (c) F. Hussain, G. R. Patzke, *CrystEngComm.*, 2011, **13**, 53; (d) W. L. Chen, Y. G. Li, Y. H. Wang, E. B. Wang, Z. M. Su, *Dalton Trans*., 2007, **38**, 4293.

10 F. Hussain, F. Conrad, G. R. Patzke, *Angew. Chem., Int. Ed.,* 2009, **48**, 9088.

11 M. Sadakane, M. H. Dickman, M. T. Pope, *Angew. Chem., Int. Ed.,* 2000, **39**, 2914.

12 C. Ritchie, E. G. Moore, M. Speldrich, P. Kögerler, and C. Boskovic, *Angew. Chem., Int. Ed.,* 2010, **49**, 7702.

13 C. Ritchie, M. Speldrich, R. W. Gable, L. Sorace, P. Kögerler and C. Boskovic, *Inorg. Chem.,* 2011, **50**, 7004.

14 X. K. Fang, T. M. Anderson, C. L. Hill, *Angew. Chem., Int. Ed.,* 2005, **117**, 3606–3610.

15 F.Y. Li, W. H. Guo and L. Xu, *Dalton Trans*., 2012, **41**, 9220.

16 B. I. D. Brown, D. Altermatt, *Inorg. Chem.* 1985, **B41**, 244.

17 J. Y. Niu, K. H. Wang, H. N. Chen, et al. *Cryst. Growth Des.,* 2009, **9**, 4362.

18 J. J. Wei, L. Yang, P. T. Ma, J. P. Wang, J. Y. Niu, *Cryst. Growth Des*., 2013, **13**, 3554.

19 (a) J.C. G. Bünzil, C. Piguet, *Chem. Rev*., 2002, **102**, 1897; b) Y. Li, F. K. Zheng, X. Liu, W. Q. Zou, G. C. Guo, C. Z. Lu, J. S. Huang, *Inorg. Chem*., 2006, **45**, 6308; (c) Z. H. Zhang, T. Okamura, Y. Hasegama, H. Kawaguchi, L. Y. Kong, Y. W. Sun, N. Ueyama, *Inorg. Chem.,* 2005, **44**, 6219; (d) W. Huang, D. Y. Wu, P. Zhou, D. Guo, C. Y. Duan, Q. J. Meng, *Cryst. Growth Des.,* 2009, **9**, 1361.

20 (a) Z. H. Zhang, Y. Song, T. Okamura, Y. Hasegawa, W. Y. Sun, N. Ueyama, *Inorg. Chem.*, 2006, **45**, 2896; (b) J. P. Costes, F. Nicodème, *Chem. Eur. J.*, 2002, **8**, 3442; (c) S. W. Zhang, Y. Wang, J. W. Zhang, P. T. Ma, J. P. Wang, J. Y. Niu, *Dalton Trans*., 2012, **41**, 3764.

21 (a) Sheldrick, G. M. *SHELXS97, Program for Crystal Structure Solution*; University of Göttingen: Göttingen, Germany, **1997**; (b) Sheldrick, G. M. *SHELXL97, Progra*m *for Crystal Structure Refinement*; University of Göttingen: Göttingen, Germany, **1997**.